Environmental Chemistry and Ecotoxicology 2 (2020) 64–72

Contents lists available at ScienceDirect

Environmental Chemistry and Ecotoxicology

journal homepage: www.keaipublishing.com/en/journals/environmental-chemistry-and-ecotoxicology/

Adsorptive removal of hazardous crystal violet dye form aqueous solution using *Rhizophora mucronata* stem-barks: Equilibrium and kinetics studies

Chrispine M. Oloo [a], John M. Onyari [a], Wycliffe C. Wanyonyi [b,*], John N. Wabomba [a], Veronica M. Muinde [a]

[a] Department of Chemistry, College of Biological & Physical Sciences, University of Nairobi, P.O. Box 30197-0 0100, Nairobi, Kenya
[b] Department of Physical Sciences, School of Science and Technology, University of Kabianga, P.O. Box 2030-20200-Kericho, Kenya

ARTICLE INFO

Article history:
Received 5 April 2020
Received in revised form 1 May 2020
Accepted 4 May 2020
Available online 8 May 2020

Keywords:
Crystal violet dye
Kinetics
Rhizophora mucronata
Equilibrium
Adsorption

ABSTRACT

Adsorption of crystal violet (CV) dye from aqueous solution using dried bark powder of mangrove species *Rhizophora mucronata* was studied. Characterization of adsorbent was done using FTIR and SEM. Batch experiment was carried out to examine the viability of using mangrove bark for adsorption of CV dye from aqueous solutions under different process conditions. The result revealed that removal of CV increased with contact time, adsorbent dose, initial dye concentration and decreased with increased particle size and ionic strength. pH 7 was the optimum pH for CV dye removal. The adsorption equilibrium for CV dye by *Rhizophora mucronata* stem-bark was attained within 60 min with removal efficacy of up to 99.8%. Pseudo-second-order kinetic model was best used to describe sorption kinetics while Freundlich isotherm model was appropriate for describing adsorption isotherm. The results demonstrated that in their raw unmodified form, *Rhizophora mucronata* stem-bark is an effective for dyes removal from industrial effluents.

1. Introduction

Organic dyes are broadly utilized to colour the finished products in industries such as cosmetics, textiles, plastic pharmaceutical, plastics, food, leather, rubber, paper etc. It is projected that about 7105 tons of 1×10^5 different dyes are manufactured global every year [1]. Wastefulness dyeing process generates coloured wastewaters that adversely pollute the environment [2]. About 10 to 15% of the synthetic dyes used in industries are discharged into environment, aggravating severe aquatic pollution [2]. The effects of these toxic colourants on the water ambiance include their propensity to prevent photosynthesis of aquatic plants by impeding permeation light, increased toxicity, COD, pH, turbidity, conductivity and BOD of the effluent. Additionally, most of these dyes cause cancer, gene mutation and can stimulate allergy and dermatitis [3–5].

Crystal violet dye (CV) is a cationic triphenyl methane dye and was used in this study as a model pollutant for adsorption studies to measure adsorption efficacy of mangrove stem barks from *Rhizophora mucronat*. The dye is well-known to be unsafe, mutagenic, carcinogenic but continually produced and consumed commercially [6]. The dye is used widely in the textile industries for dying cotton, wool, silk, nylon, print for making inks, biological staining, and as a dermatological agent in veterinary medicine [7–9]. CV is among the brightest water-soluble class of dye and a concentration of <1.0 mg/l can induce an intense coloration that has an inhibitory influence on photosynthesis. The dye can be absorbed through the skin, inhalation and ingestion causing horrible irritation and painful sensitization [9]. Kidney failure, acute eye inflammation that can lead to permanent blindness and cancer occurs in extreme cases. Due to public outcry and negative health effects of dye contaminated wastewaters, governments have been forced to establish rigid laws on permissible pollutants concentration discharged by industries.

Treatment of wastewaters contaminated with organic dyes is a difficult and costly procedure since dyes are made up of complex aromatic structure stable to oxidizing agents, light, water, heat, and microbial attack [1]. Over the last few decades, different, conventional treatment methods like precipitation [10] photo-catalytic decolourization [1] coagulation and flocculation [11], membrane separation [12], activated carbon [13] photocatalytic, adsorption and electrochemical [14] and biological degradation [4] have been examined with varying levels of success. Adsorption has shown to be superior compared to other techniques used in the dye removal in effluent because of its ease in design, diversity in uses and low amount of unsafe secondary products [15]. Commercial activated carbon has proved to be an excellent adsorbent but it's high cost with respect to activation, regeneration and rapid saturation make it less economically viable [16]. This drawbacks have necessitated diverse studies to search for cheap, eco-friendly and effective auxiliary adsorbent materials such as palm fibre [17], coconut husks [18], zinc sulphide [19], potato-peels [20], chitosan films [21] among others.

* Corresponding author.
E-mail address: wwanyonyi@kabianga.ac.ke. (W.C. Wanyonyi).

Production and hosting by Elsevier on behalf of KeAi

http://dx.doi.org/10.1016/j.enceco.2020.05.001

Ecological habitats occupied by mangroves are a unique ecosystem exemplified by numerous stress conditions such as water logging, high salinity, low nutrition condition, light stress and low oxygen condition, normally found in abundant along the coastal regions of East Africa, India, South East Asia and Australia [22]. Mangroves forms a vital coastal ecosystem and apart from shoreline protection, waste assimilation and carbon sequestration among other importance of the mangrove plant; fishes, some amphibians and other fauna also inhabit these forests as breeding grounds and habitat [23]. Among the nine mangrove species along the Kenyan coastline, *Rhizophora mucronata*, *Xylocarpus moluccensis* and *Ceriops tagal* are the dominant species contributing up to 70% of the 54,000 *ha* mangrove forests formation [24]. Globally, mangroves provide diverse forms of goods and services for instance furniture, fuelwood, building boats and houses, honey, tannins, medicinal plants and habitation for marine species targeted in commercial, recreational, and subsistence fisheries [25,26]. Mangrove Stem-Barks are largely discarded when processing furniture, timbers and boats. This industrial residue is mostly burned for energy production or simply thrown away on land without any economic value causing environmental pollution. Population increase in East Africa in recent years has put pressure on land use leading to deforestation of the vital mangrove forest [26]. This study affords an opportunity to demonstrate the important role played by mangroves species in phytoremediation process of pollutants such as dyes that may be discharged into Marine ecosystems and recommend increased conservation and reafforestation programs along coastal areas to protect the environment. The efficiency of dried Stem-Barks powder in adsorption of CV dye was analyzed and factors affecting adsorption optimized.

2. Materials and methods

2.1. Materials

Fresh mangrove stem barks from *Rhizophora mucronat* (RM) species was collected from Gazi Bay, Kwale County, Kenya. They were cleaned with tap water to eliminate water soluble impurities and foreign particles. The materials were dried on sun for two weeks and then crushed into powder. The powder was extensively washed with distilled water before drying in an oven at 60 °C for 36 h. The dried powders were stored in sealed plastic bags awaiting adsorption studies. The dried biomass was subsequently used for surface characterization and adsorption studies. The crystal violet (CV) dye of analytical grade was purchased from Manigate Agencies LTD and subjected to adsorption experiments without further purification.

2.2. Characterization

Fourier Transform Infrared Spectrophotometer, (IRAffinity-1S FTIR-Shimadzu model) was used to identify functional groups on *Rhizophora mucronat* stem-barks. The fine powder was thoroughly cleaned using distilled water. The raw samples were mixed with potassium bromide (KBr) powder, at an approximate ratio of 1/200, triturated then made into a 1 mm pellets for FTIR analysis at frequency range of 4000–400 cm^{-1}. Graphical results were then interpreted to ascertain the key compounds present in the matrix of the materials. Transmission electron microscopes (SEM) (2100, JEOL, Japan) was applied to evaluate the morphological microstructure of the *Rhizophora mucronat* stem-barks.

2.3. Batch adsorption experiments

Batch adsorption experiments were executed in triplicate in a 250 mL Erlenmeyer flask placed on an orbital shaker (Thermolyne-type 65,800) set at optimum condition of 150 rpm as reported [27]. The influence of contact time was determined by mixing 0.25 g of *Rhizophora mucronat* stem-barks powder of particle size >300 μm < 425 μm into 40 mL of CV dye at 25 °C. Aliquots were drawn from mixture after 5-minute time interval upon which the concentration of CV dye measured using UV/Vis spectrophotometer at maximum wavelength (λ_{max} = 590 nm). Similarly, influence of adsorbent dose on sorption of CV dye was examined using 0.125, 0.250, 0.375 and 0.500 g of mangrove stem barks powder at 25 °C while initial dye concentration influence was assessed by changing CV dye concentration from 2.50×10^{-6} to 2.50×10^{-5} M. pH effect was determined by changing the CV dye pH from 2 to 10. 1 M NaCl concentrations were used determine the impact of ionic strength on adsorption. Particle size impact was determined by mixing 0.25 g of particle size >70 μm < 300 μm; > 300 μm < 425 μm; and >425 μm < 812 μm with 40 mL of 2.50×10^{-5} M CV dye. Solutions pH was regulated by 0.1 M NaOH or 0.1 M HCl as required. CV dye adsorbed per unit mass of *Rhizophora mucronat* stem-barks was work out using Eq. (1):

$$q_e = \frac{V(C_o - C_e)}{W} \quad (1)$$

where C_o and C_e refers to the initial and equilibrium CV dye concentrations (mg/g), V is the volume of dye solution (L) and W is the quantity of adsorbent used (g). Percent dye removed (%) was computed using Eq. (2):

$$\%\text{dye } Removed = \frac{(C_o - C_e)}{C_o} \times 100\% \quad (2)$$

Adsorption isotherms and kinetics of dye removal was investigated using variable CV dye concentration at 25 °C, 0.25 g of *Rhizophora mucronat* stem-barks powder of particle size 70–300 μm was mixed with 40 mL CV dye solution in 250 mL conical flasks quivering at 150 rpm. Aliquots of 3 mL were drawn at 10-minute time intervals and the remaining CV dye concentration determined.

3. Results and discussion

3.1. SEM analysis

The scanning electron microscope (SEM) was employed to evaluate the surface physical morphology of *Rhizophora mucronata* stem-bark at ×300 magnifications before and after adsorption and the results displayed in Fig. 1A and B. The results show a porous structure with irregular rough surface full of small pores with cavities. The surface features of the *Rhizophora mucronata* stem-bark further expose non-linear grooves and projections that are responsible for the increased surface area suitable for large adsorption capacity [28,29]. Considering the multi-porous structure of *Rhizophora mucronata* stem-bark, the dissolved CV dye molecules can lightly permeate into the interior, thus enhancing the adsorption ability. The surface morphology predicts adsorption of CV dye may have occurred through diffusion process. After adsorption (Fig. 1B), the biomaterial surface on average appeared relatively smooth but numerous micro and macro pores generally remained open continuing to make available access to the inner of the fibre. These observations further suggest that CV dye adsorbed onto the surface of *Rhizophora mucronata* stem-bark powder forming a thin layer.

3.2. FTIR analysis

FTIR study was done to ascertain the core functional group present on the surface of *Rhizophora mucronata* stem back responsible for dye binding. Fig. 2 shows the FTIR spectrum of *Rhizophora mucronata* stem-bark before and after adsorption. FTIR spectrum of *Rhizophora mucronata* stem-bark exhibited broad absorption peak at 3242.34 cm^{-1} referring to stretching vibration of hydroxyl groups from a phenol or alcohol. The peaks observed at 2918.30 is due to stretching vibration of aliphatic (SP^3) hydrocarbon (-CH) groups while the peak at 1602.85 cm^{-1} is characteristic of aromatic CC bending. The strong peak at 1026.13 cm^{-1} is due to CO stretching in phenols, ethers and esters [30]. After adsorption, the peaks broaden and a new peak is observed at 2349.30 cm^{-1} suggesting the formation of new CH stretching which causes the vibrations of CH, CH_2, and CH_3 groups [31]. The presence of –OH group and the carbonyl indicate a possible

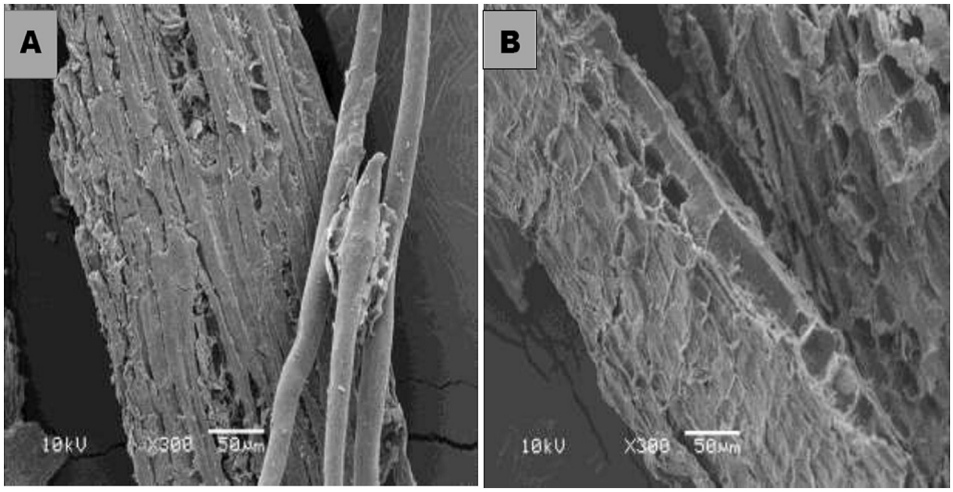

Fig. 1. SEM images of *Rhizophora mucronata* stem-bark sample (A) before adsorption and (B) after adsorption.

carboxylic group. The shifting of peaks for example, the peaks at 2216.21 cm^{-1} shifted to 2349.30 cm^{-1} after adsorption of CV dye shows that a new bond has been created. It is evident that the surface hydroxyl groups of the adsorbent played an important role in the adsorption process. These results are characteristic of the chemical groups present in lignin, hemicelluloses, and cellulose, which are the key constituents of *Rhizophora mucronata* stem-bark [2].

3.3. Effect contact time

Contact time regulates equilibrium kinetics, emphasises on the stability of the adsorption process and gives an outlook of the general cost considered when designing the sorption system for large scale use [32,33]. Contact time influence on CV dye uptake was performed at 25 °C and the findings displayed in Fig. 3a. The rate of adsorption increase with time then slowed down after 10 min as the system attains equilibrium due to exhaustion of the adsorptive sites [34]. Percentage change in dye uptake after the 5th minute was relatively gradual with the equilibrium being reached within 60 min with 99.8% dye removal. This verifies a higher number of sorption sites on the bark as observed by [35].

3.4. Effect of adsorbent dose

Fig. 3b displays adsorbent dose effect of on adsorptive removal of CV dye. The results revealed that the quantity of CV dye removed per unit mass of *Rhizophora mucronata* stem-bark at equilibrium increased with increase in the dose. It is evident that the optimum dose for adsorption is 0.25 g, beyond 0.5 g a relatively constant adsorption performance was witnessed. The increased dye removal with increase in *Rhizophora*

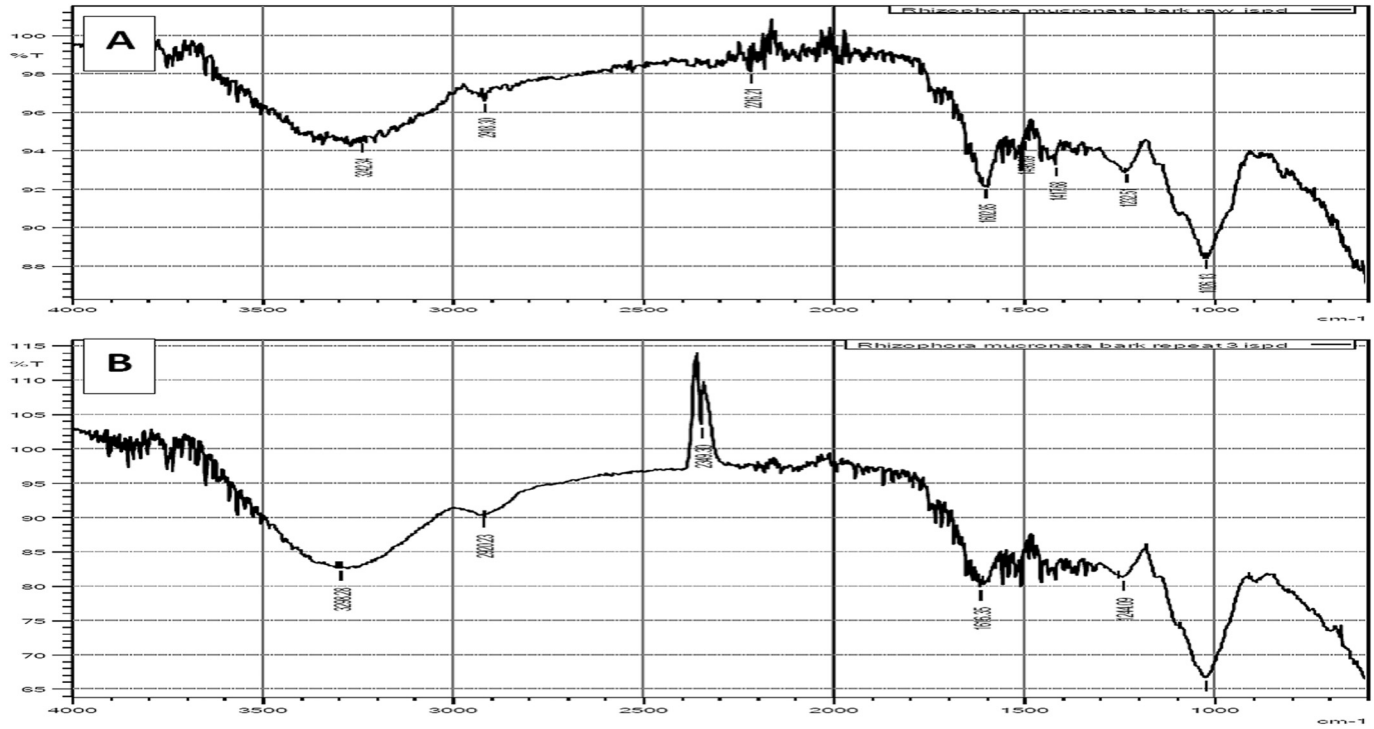

Fig. 2. FTIR spectrum of *Rhizophora mucronata* stem-bark: (A) before adsorption (B) after adsorption of CV dye.

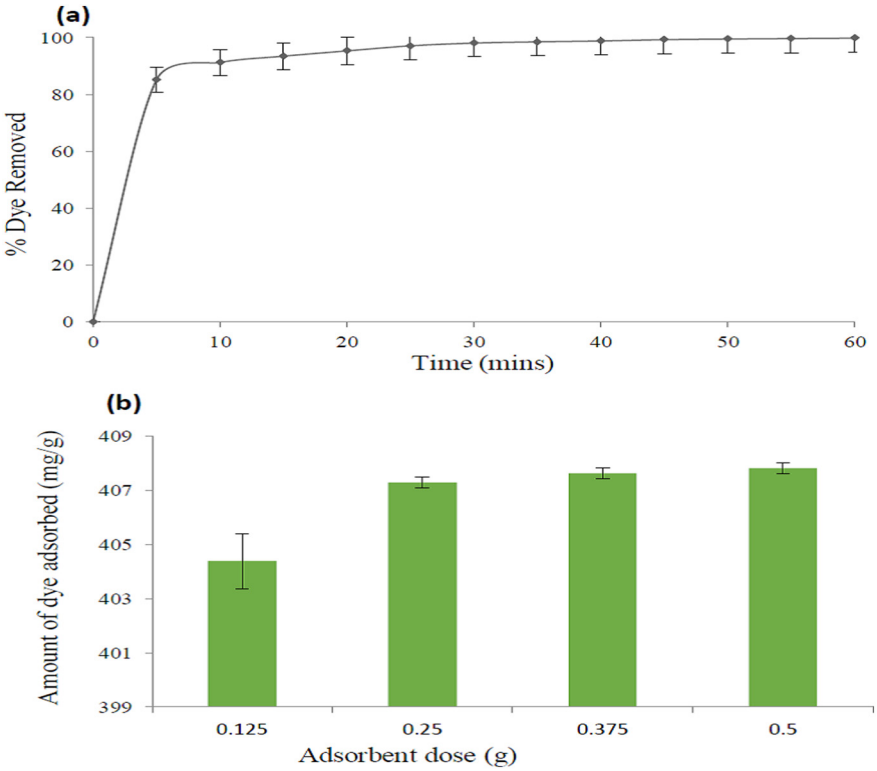

Fig. 3. (a) Contact time effect on adsorption of CV dye, (b) adsorbent dose effect on adsorption of CV dye onto *Rhizophora mucronata* stem-bark (RM: 0.25 g/40 mL of 2.50×10^{-5} M, at 25 °C, pH 7).

mucronata stem-bark dose is ascribed to increased adsorbent surface area accessible by dye molecule due to increased mass [36]. However a limit is reached at which no more adsorption occurs as the quantity of the adsorbent increases due to the overlapping particles active sites and this reduces the efficiency of the process [37].

3.5. Effect of initial CV dye concentration

The initial dye concentration effect on adsorption of CV dye is shown in Fig. 4 a. The result revealed that the quantity of dye adsorbed rose when dye concentration increased. Whereas the sorption process is dependable on the concentration of the dyes, at very low CV dye concentration, fractional adsorption is low and the adsorption process is not dependent on the initial dye concentration. However larger fractional adsorption ratio is realized at higher concentrations [38]. Moreover, the actual available sites for adsorption become fewer at higher concentrations since the dye molecules overlap over these sites. Consequently, the quantity of dye being adsorbed decreases and hence the adsorption capacity obtained is low [39].

3.6. Effect of the particle size

Adsorption is a surface phenomenon which depends on the available surface area on the adsorbent and therefore characterization of particle sizes of the materials is important [27,40]. Higher % dye removal was achieved using smaller particle sizes size (>70 < 300 μm) of the adsorbent material since they provide large surface area in comparison to large particle sizes (>425 μm < 812 μm) as illustrated in Fig. 4b. Smaller particle sizes provide a large surface area which reflects an increased number of surface active sites than lumpy particle sizes. The obtained results concur with similar findings obtained in the adsorption of crystal violet dye on coffee husks [16].

3.7. Effect of ionic strength

The cations and anions present in textile and other industrial effluents affect the concentration of ion in the effluent impacting the treatment process. Ionic strength effect on removal of CV was determined by varying the concentration of the 1.0 M NaCl and the result presented in Fig. 5a. The sorption efficiency of *Rhizophora mucronata* stem-bark diminished with rise in ionic strength of the aqueous mixture. At higher concentrations of the NaCl, a tremendous decrease of about 6.72% was witnessed. The ionic strength is a measure of the rate at which the cationic and anionic characters in the aqueous mixture compete for the available active sites and this results to a decreased quantity of adsorbed dye per unit adsorbent mass [18]. A higher concentration of Na^+ would viciously compete for the available sites out numbering the cationic dyes particles at molecular level, leading to a sorption decrease. Furthermore, the Na^+ ions are smaller in size than the dye molecules (in which there are quite a number of groups causing screening effect); and will swiftly access the anionic sites on the surface of *Rhizophora mucronata* stem-bark. Similar findings on reduction of dye removal with increase in ionic strength have been reported [41,42].

3.8. Effect of pH

pH plays crucial function by regulating the charge on adsorbent, surface characteristic, the level of adsorbate ionization and dissociation of different functional groups. Wastewaters from textile industries have broad range of pH that depends on the type of dye and reagents applied. Fig. 5b. shows the variation in CV dye adsorption with change in the initial pH of the solution. It is clear that an upsurge in pH caused an increase dye removal up to an optimum value of pH 7, after which, there was a slightly reduction in adsorption. This tendency can be attributed to the rise of negative charge density on adsorbent in acidic pH solutions [43], causing attraction between the positively charged CV dye molecule and *Rhizophora mucronata* stem-bark. As the pH rose, the surfaces charge density on the adsorbent declined,

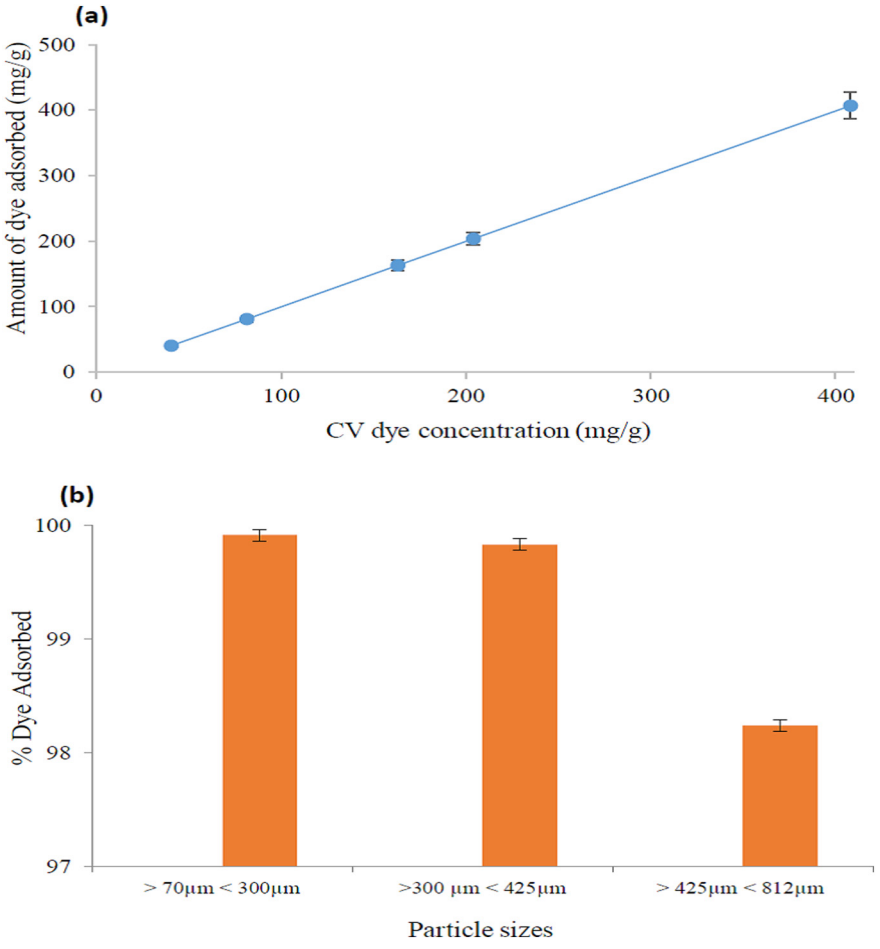

Fig. 4. (a) Initial dye concentration effect on adsorption CV dye, (b) particle size effect on adsorption of CV dye onto *Rhizophora mucronata* stem-bark (RM: 0.25 g/40 ml, CV: 1.0×10^{-5}M, at 25 °C, pH 7).

resulting in electrostatic repulsion from the positive charge of the dye molecule [17].

3.9. Kinetic studies

A literal interpretation of the model entails presumptions that different adsorption sites on a solid substrate randomly collide with each other during a rate-limiting mechanistic step [44]. The experimental data were modelled by pseudo-first and second order models. A pseudo first order reaction is one which is literally a second order but the concentration of one of the reactants is in excess rendering the overall order a first order reaction. The pseudo-first order kinetics equation [45] is given by Eq. (3):

$$Log\ (q_e - q_t) = \ logq_e - \frac{tk_1}{2.303} \tag{3}$$

where k_1 is the rate constant of pseudo-first-order adsorption, q_e and q_t are the quantities of dye removed by *Rhizophora mucronata stem-bark* at equilibrium and at time, t, respectively. Fig. 6a presents pseudo-first-order kinetics plot for the sorption of CV dye on *Rhizophora mucronata* stem-bark. The rate constants, projected dye uptakes at equilibrium and the corresponding correlation coefficients were determined and given in Table 1.

The pseudo-second-order kinetic model was also used to estimate adsorption kinetics of CV dye on *Rhizophora mucronata* stem-bark. The pseudo second-order model [46] is stated by Eq. 4.

$$\frac{t}{q_t} = \frac{1}{k_2}.\frac{1}{q^2_e} + \frac{t}{q_e} \tag{4}$$

where k_2 is the rate constant for pseudo-second-order ($gmg^{-1}\ min^{-1}$). A graph of t/q_t vs t yields a straight line, where, q_e and k_2 are determined from the gradient and intercept of the plot. Fig. 6b shows pseudo second order kinetics plot for sorption of CV dye by *Rhizophora mucronata* stem-bark. The constant k_2 and R^2 are listed in Table 1. Experimental data demonstrated good agreement with the pseudo-second-order equation with high R^2 value of 0.9998 providing evidence that the adsorption of CV on *Rhizophora mucronata* stem-bark followed pseudo-second-order kinetic model. The two contributing explanations for these results are (a) significant depletion of the bulk dye concentration during a batch adsorption experiment, and (b) the requirement for longer periods of time for adsorbing species to diffuse to remote locations deep within a network of fine pores [44]. The results reveals that sorption of CV dye occurs possibly through surface interchange reactions till all active sites are fully covered; thereafter dye particles disperse through the adsorbent complex for more interaction [47]. Similar kinetics was also observed in adsorption of methylene blue by coconut husks/polylactide blended films [33], adsorption of CV dye on zeolites from coal fly and bottom ashes [9] and adsorption of CV dye on coffee husks [16].

3.10. Adsorption isotherms

Adsorption isotherms describe how adsorbent and adsorbate materials interact and so, it is critical in optimizing the treatment process [47]. It is imperative to determine the best relationship for the equilibrium curve for optimum design of an adsorption system. Adsorption isotherms of *Rhizophora mucronata* stem-bark were analyzed using the Langmuir [48] and Freundlich [49] equation. The linearized form of the Langmuir

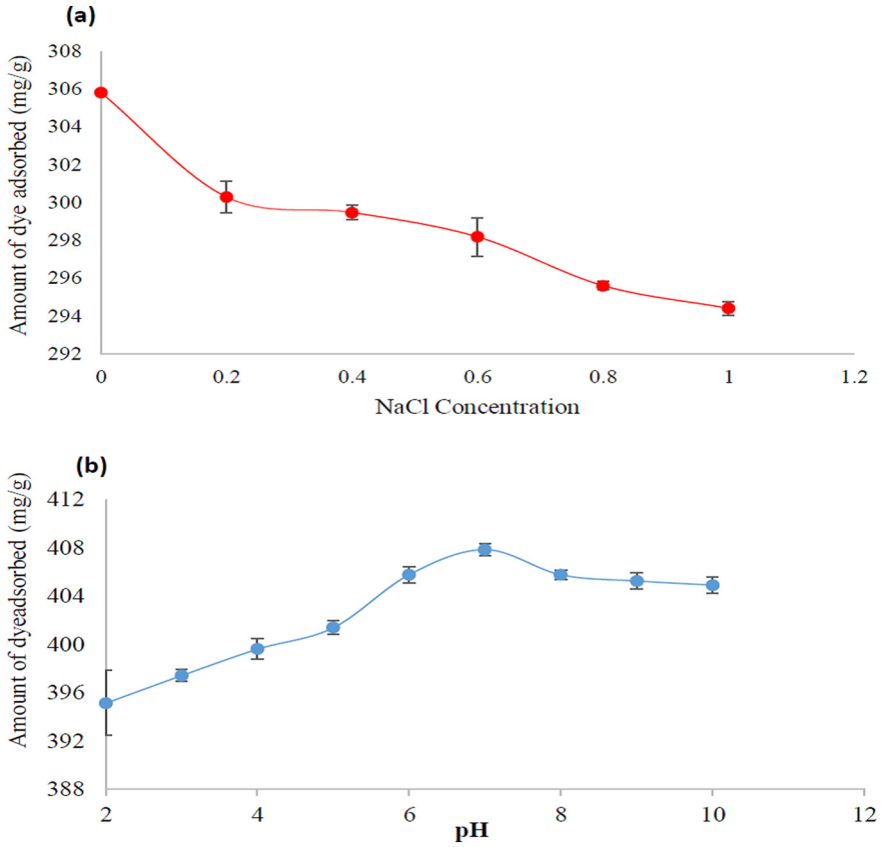

Fig. 5. (a) Ionic strength effect on adsorption of CV dye, (b) effect of pH on adsorption of CV dye onto *Rhizophora mucronata* stem-bark (CV: 1.0 × 10^{-5}M, RM: 0.25 g/40 ml, at 25 °C).

equation is given as:

$$\frac{C_e}{Q_e} = \frac{1}{K_L Q_m} + \frac{C_e}{Q_m} \quad (5)$$

where Q_e is the adsorbate quantity at equilibrium (mg/g), Q_m is maximum monolayer adsorption capacity of the adsorbent (mg/g), C_e is equilibrium concentration of adsorbate (mg/l) and K_l is the Langmuir adsorption constant related to the free energy adsorption (l/mg). The Langmuir constant Q_m and K_L values are calculated from the gradient and intercept

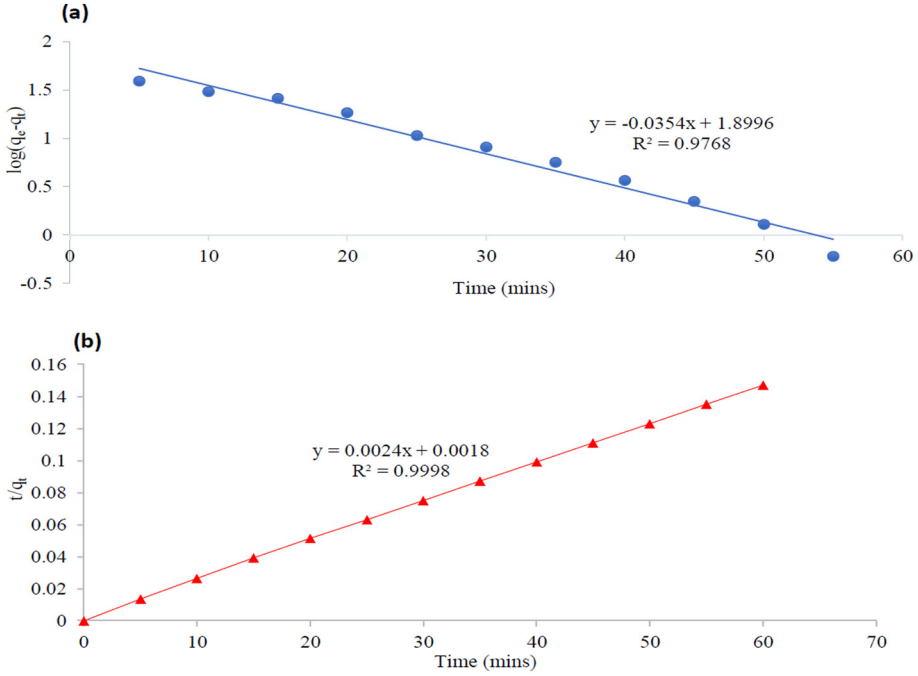

Fig. 6. (a) Pseudo-first order kinetics for CV dye adsorption, (b) pseudo-second kinetics for CV dye adsorption onto *Rhizophora mucronata* stem-bark.

Table 1
Kinetic modelling data for adsorption of crystal violet dye by *Rhizophora mucronata* stem-bark.

Pseudo-first-order				Pseudo-second-order		
$q_{e.\ exp}$ (mg/g)	$q_{e.cal}$ (mg/g)	k_1 (g/mg min)	R^2	$q_{e.cal}$ (mg/g)	k_2 (g mg^{-1} min)	R^2
407.2990	486.6587	0.0815	0.9768	416.6667	0.0033	0.9998

respectively, of linear plot of C_e/Q_e verses C_e (Fig. 7a). A separation factor of equilibrium parameter, R_L, illustrates important features of Langmuir isotherm model. It can be worked out by Eq. (6).

$$R_L = \frac{1}{1 + C_o K_L} \tag{6}$$

where C_0 is the initial dye concentration of the adsorbate (mg/l). Values of R_L indicate the shapes of isotherms to be either unfavorable ($R_L > 1$), linear ($R_L = 1$), favorable ($0 < R_L < 1$). From the plot, the corresponding Langmuir isotherm constants were determined. The result reveals that mono layer adsorption capacity (Q_m) of 1.1809 mg/g was achieved with Langmuir constant K_L of 1.8978 Lmg, R^2 values of 0.8783 and R_L value of 0.4462. Freundlich isotherm which presumes multilayer sorption on heterogeneous adsorbent surface was also used to evaluate experimental data. The linearized form of the equation is given as:

$$\text{Log } Q_e = \text{Log } K_f + \frac{1}{n} \log C_e. \tag{6}$$

where K_f (l/g) is Freundlich constant, indicating the adsorption capacity and n is the Freundlich exponent that illustrates the adsorption intensity. The magnitude of the exponent, 1/n, gives an indication of the favorability of adsorption. Values of $n > 1$ represent favorable adsorption conditions [50]. A plot of log Q_e vs log C_e is linear with K_f and η obtained from the intercepts and the slope respectively (Fig. 7b). The corresponding Freundlich constants were determined. The results showed that Freundlich constant related to adsorption capacity (k_f) of 0.6584 (mg/g) (l/mg) was achieved with adsorption intensity (n) value of 0.5269 and R^2 value of 0.9930. Experimental values showed relatively better fit to the Langmuir adsorption isotherm model and the dimensionless parameter RL ranged between zero and one ($0 < R_L < 1$) indicating favorable adsorption process. However, considering high value of R^2, Freundlich model, it can be established that multilayer adsorption processes was dominant and thus Freundlich adsorption isotherm model is best used to describe adsorption of CV dye onto *Rhizophora mucronata* stem-bark with adsorption capacity of 0.6584 mg/g. Similar conclusions have been reported on the sorption of Acid Blue 161 by defatted micro-algal biomass and removal of Reactive black 5 dye by Macadamia Seed Husks where adsorption capacity of 14.199 and 4.20679 mgg^{-1} were achieved respectively [5,51].

4. Conclusion

The study establishes that *Rhizophora mucronata stem-bark* is certainly feasible, low-cost adsorbent for the adsorption of CV dye from effluent with over 99.8% efficiency. Results revealed that adsorption of CV dye onto *Rhizophora mucronata* stem-bark strongly controlled by time of contact, ionic strength, dye concentration, dosage and particle size. SEM image showed that *Rhizophora mucronata* stem-bark consists of porous structure with irregular rough surface full of cavities which provide perfect state for adsorption. The quantity of dye uptake (mg/g) was found to rise with increase in dye concentration and adsorbent dose but reduced with rise in ionic strength and particle size. pH 7 was found to be the optimum pH for dye removal. The results obtained showed that Freundlich isotherm model gave the best fit to the experimental data with higher correlation coefficients ($R^2 = 0.993$) suggesting t multi-layer adsorption process. R_L value showed that adsorption was favorable. Experimental data followed pseudo-second-order kinetics with high correlation coefficient ($R^2 = 0.9998$). Subsequently, it can be concluded that *Rhizophora mucronata* stem-bark can be used as a low-cost, efficacious alternate material for CV dye removal in effluent.

CRediT authorship contribution statement

Chrispine M. Oloo: Investigation, Writing - original draft, Funding acquisition.**John M. Onyari:**Conceptualization, Supervision, Resources. **Wycliffe C. Wanyonyi:**Conceptualization, Methodology, Software, Data curation, Supervision, Writing - review & editing, Software, Validation,

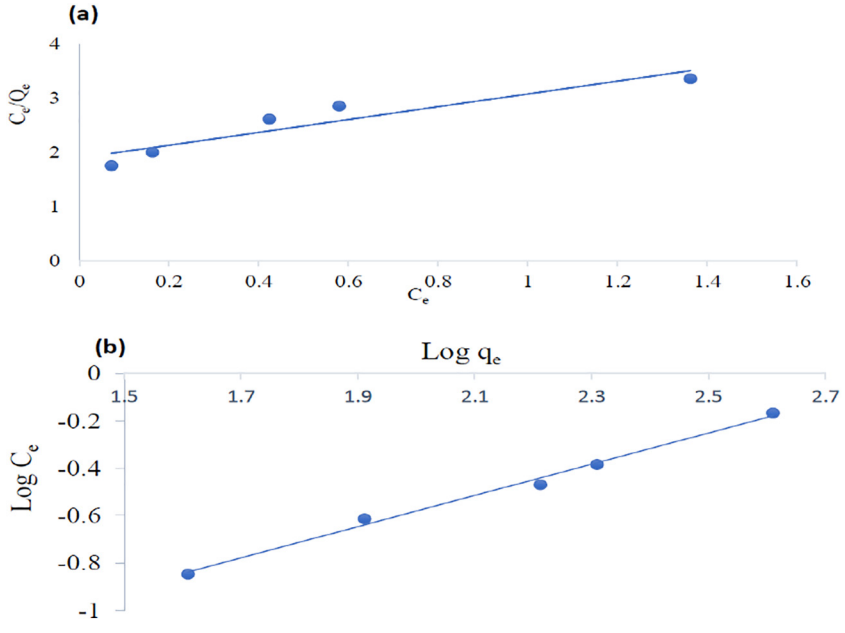

Fig. 7. (a) Langmuir Isotherm for CV dye adsorption, (b) Freundlich Isotherm for CV dye adsorption onto *Rhizophora mucronata* stem-bark.

Funding acquisition, Resources, Formal analysis, Visualization.**John N. Wabomba:**Supervision, Visualization.**Veronica M. Muinde:**Visualization.

Declaration of competing interest

We want to declare that this paper has no competing interests to declare.

Acknowledgements

The author would like to acknowledge financial assistance provided by University of Kabianga research grants and National Research Fund (NRF) Grant provided by Government of Kenya.

References

[1] U. Roy, S. Manna, S. Sengupta, P. Das, S. Datta, A. Mukhopadhyay, A. Bhowal, Dye removal using microbial biosorbents, in: G. Crini, E. Lichtfouse (Eds.), Green Adsorbents for Pollutant Removal, Springer International Publishing, Cham 2018, pp. 253–280, https://doi.org/10.1007/978-3-319-92162-4_8.

[2] J.N. Wekoye, W.C. Wanyonyi, P.T. Wangila, M. Tonui, Kinetic and equilibrium studies of Congo red dye adsorption on cabbage waste powder, Environmental Chemistry and Ecotoxicology S2590182620300047 (2020)https://doi.org/10.1016/j.enceco.2020.01.004.

[3] N.F. Cardoso, E.C. Lima, B. Royer, M.V. Bach, G.L. Dotto, L.A.A. Pinto, T. Calvete, Comparison of Spirulina platensis microalgae and commercial activated carbon as adsorbents for the removal of Reactive Red 120 dye from aqueous effluents, J. Hazard. Mater. 241–242 (2012) 146–153, https://doi.org/10.1016/j.jhazmat.2012.09.026.

[4] W.C. Wanyonyi, J.M. Onyari, P.M. Shiundu, F.J. Mulaa, Biodegradation and detoxification of malachite green dye using novel enzymes from Bacillus cereus strain KM201428: kinetic and metabolite analysis, Energy Procedia 119 (2017) 38–51, https://doi.org/10.1016/j.egypro.2017.07.044.

[5] M.M. Felista, W.C. Wanyonyi, O. Gilbert, Adsorption of anionic dye (Reactive Black 5) using macadamia seed husks: kinetics and equilibrium studies, Scientific African (2020)https://doi.org/10.1016/j.sciaf.2020.e00283 e00283.

[6] G.K. Sarma, S. Sen Gupta, K.G. Bhattacharyya, Adsorption of crystal violet on raw and acid-treated montmorillonite, K10, in aqueous suspension, J. Environ. Manag. 171 (2016) 1–10, https://doi.org/10.1016/j.jenvman.2016.01.038.

[7] A. Adak, M. Bandyopadhyay, A. Pal, Removal of crystal violet dye from wastewater by surfactant-modified alumina, Sep. Purif. Technol. 44 (2005) 139–144, https://doi.org/10.1016/j.seppur.2005.01.002.

[8] L. Ayed, K. Chaieb, A. Cheref, A. Bakhrouf, World J. Microbiol. Biotechnol. 25 (2009) 705–711, https://doi.org/10.1007/s11274-008-9941-x.

[9] T.C.R. Bertolini, J.C. Izidoro, C.P. Magdalena, D.A. Fungaro, Adsorption of crystal violet dye from aqueous solution onto zeolites from coal fly and bottom ashes, 14 (2013).

[10] C. Shen, Y. Pan, D. Wu, Y. Liu, C. Ma, F. Li, H. Ma, Y. Zhang, A crosslinking-induced precipitation process for the simultaneous removal of poly (vinyl alcohol) and reactive dye: the importance of covalent bond forming and magnesium coagulation, Chem. Eng. J. 374 (2019) 904–913, https://doi.org/10.1016/j.cej.2019.05.203.

[11] M. Kilic, E. Apaydin-Varol, A.E. Pütün, Adsorptive removal of phenol from aqueous solutions on activated carbon prepared from tobacco residues: equilibrium, kinetics and thermodynamics, J. Hazard. Mater. 189 (2011) 397–403, https://doi.org/10.1016/j.jhazmat.2011.02.051.

[12] H. Liu, Y. Chen, K. Zhang, C. Wang, X. Hu, B. Cheng, Y. Zhang, Poly(vinylidene fluoride) hollow fiber membrane for high-efficiency separation of dyes-salts, J. Membr. Sci. 578 (2019) 43–52, https://doi.org/10.1016/j.memsci.2019.02.029.

[13] M. Hasanzadeh, A. Simchi, H. Shahriyari Far, Nanoporous composites of activated carbon-metal organic frameworks for organic dye adsorption: synthesis, adsorption mechanism and kinetics studies, J. Ind. Eng. Chem. 81 (2020) 405–414, https://doi.org/10.1016/j.jiec.2019.09.031.

[14] M.S. Anantha, S. Olivera, C. Hu, B.K. Jayanna, N. Reddy, K. Venkatesh, H.B. Muralidhara, R. Naidu, Comparison of the photocatalytic, adsorption and electrochemical methods for the removal of cationic dyes from aqueous solutions, Environ. Technol. Innov. 17 (2020) 100612, https://doi.org/10.1016/j.eti.2020.100612.

[15] N.A. Khan, S.H. Jhung, Adsorptive removal and separation of chemicals with metal-organic frameworks: contribution of π-complexation, J. Hazard. Mater. 325 (2017) 198–213, https://doi.org/10.1016/j.jhazmat.2016.11.070.

[16] G.K. Cheruiyot, W.C. Wanyonyi, J.J. Kiplimo, E.N. Maina, Adsorption of toxic crystal violet dye using coffee husks: equilibrium, kinetics and thermodynamics study, Scientific African 5 (2019), e00116. https://doi.org/10.1016/j.sciaf.2019.e00116.

[17] M. Alshabanat, G. Alsenani, R. Almufarij, Removal of crystal violet dye from aqueous solutions onto date palm fiber by adsorption technique, Journal of Chemistry. 2013 (2013).

[18] S. Ali, J.M. Onyari, J.N. Wabomba, Comparative Adsorption of Methylene Blue and Congo Red Dyes Onto Coconut Husks, Mangrove and Polyactide Blended Films, Ali et al. 2014.

[19] M. Dastkhoon, M. Ghaedi, A. Asfaram, A. Goudarzi, S.M. Langroodi, I. Tyagi, S. Agarwal, V.K. Gupta, Ultrasound assisted adsorption of malachite green dye onto ZnS: Cu-NP-AC: equilibrium isotherms and kinetic studies–response surface optimization, Sep. Purif. Technol. 156 (2015) 780–788.

[20] S. Lairini, K.E. Mahtal, Y. Miyah, K. Tanji, S. Guissi, S. Boumchita, F. Zerrouq, The adsorption of Crystal violet from aqueous solution by using potato peels (*Solanum tuberosum*): equilibrium and kinetic studies, 10 (2017).

[21] G.L. Dotto, L.A.A. Pinto, M.A. Hachicha, S. Knani, New physicochemical interpretations for the adsorption of food dyes on chitosan films using statistical physics treatment, Food Chem. 171 (2015) 1–7, https://doi.org/10.1016/j.foodchem.2014.08.098.

[22] I.W. Hendy, L. Michie, B.W. Taylor, Habitat creation and biodiversity maintenance in mangrove forests: teredinid bivalves as ecosystem engineers, PeerJ. 2 (2014), e591. https://doi.org/10.7717/peerj.591.

[23] N. Thomas, R. Lucas, P. Bunting, A. Hardy, A. Rosenqvist, M. Simard, Distribution and drivers of global mangrove forest change, 1996–2010, PLoS One 12 (2017), e0179302. https://doi.org/10.1371/journal.pone.0179302.

[24] S.S. Romañach, D.L. DeAngelis, H.L. Koh, Y. Li, S.Y. Teh, R.S. Raja Barizan, L. Zhai, Conservation and restoration of mangroves: global status, perspectives, and prognosis, Ocean Coast. Manag. 154 (2018) 72–82, https://doi.org/10.1016/j.ocecoaman.2018.01.009.

[25] J.K. Lang'at, J.G. Kairo, Conservation and Management of Mangrove Forests in Kenya, 2008.

[26] C.M. Beitl, P. Rahimzadeh-Bajgiran, M. Bravo, D. Ortega-Pacheco, K. Bird, New valuation for defying degradation: visualizing mangrove forest dynamics and local stewardship with remote sensing in coastal Ecuador, Geoforum. 98 (2019) 123–132, https://doi.org/10.1016/j.geoforum.2018.10.024.

[27] W.C. Wanyonyi, J.M. Onyari, P.M. Shiundu, Adsorption of Congo red dye from aqueous solutions using roots of Eichhornia crassipes: kinetic and equilibrium studies, Energy Procedia 50 (2014) 862–869, https://doi.org/10.1016/j.egypro.2014.06.105.

[28] M.H. Abu Elella, M.W. Sabaa, E.A. ElHafeez, R.R. Mohamed, Crystal violet dye removal using crosslinked grafted xanthan gum, Int. J. Biol. Macromol. 137 (2019) 1086–1101, https://doi.org/10.1016/j.ijbiomac.2019.06.243.

[29] S. Manna, D. Roy, P. Saha, D. Gopakumar, S. Thomas, Rapid methylene blue adsorption using modified lignocellulosic materials, Process. Saf. Environ. Prot. 107 (2017) 346–356, https://doi.org/10.1016/j.psep.2017.03.008.

[30] V.M. Muinde, J.M. Onyari, B. Wamalwa, J. Wabomba, R.M. Nthumbi, Adsorption of malachite green from aqueous solutions onto rice husks: kinetic and equilibrium studies, J. Environ. Prot. 8 (2017) 215–230, https://doi.org/10.4236/jep.2017.83017.

[31] Z. Mat Lazim, N.S. Zulkifli, T. Hadibarata, Z. Yusop, Removal of Cresol red and Reactive Black 5 dyes by using spent tea leaves and sugarcane baggase powder, Jurnal Teknologi 74 (2015)https://doi.org/10.11113/jt.v74.4884.

[32] A.M. Aljeboree, et al., A.F. Alkaim, A.H. Al-Dujaili, Adsorption isotherm, kinetic modeling and thermodynamics of crystal violet dye on coconut husk-based activated carbon, Desalin. Water Treat. 53 (2015) 3656–3667.

[33] A. Shee, J.M. Onyari, J.N. Wabomba, D. Munga, Methylene blue adsorption onto coconut husks/polylactide blended films: equilibrium and kinetic studies, Chemistry and Materials Research 6 (2014).

[34] T.S. Anirudhan, S.S. Sreekumari, Adsorptive removal of heavy metal ions from industrial effluents using activated carbon derived from waste coconut buttons, J. Environ. Sci. 23 (2011) 1989–1998, https://doi.org/10.1016/S1001-0742(10)60515-3.

[35] M.T. Yagub, T.K. Sen, S. Afroze, H.M. Ang, Dye and its removal from aqueous solution by adsorption: a review, Adv. Colloid Interf. Sci. 209 (2014) 172–184.

[36] G. Crini, H. Peindy, F. Gimbert, C. Robert, Removal of C.I. basic green 4 (malachite green) from aqueous solutions by adsorption using cyclodextrin-based adsorbent: kinetic and equilibrium studies, Separation and Purification Technology 53 (2007) 97–110, https://doi.org/10.1016/j.seppur.2006.06.018.

[37] K. Jedynak, M. Repelewicz, Adsorption of methylene blue and malachite green on micro-mesoporous carbon materials, Adsorpt. Sci. Technol. 35 (2017) 499–506, https://doi.org/10.1177/0263617417698706.

[38] S. Chakraborty, S. Chowdhury, P.D. Saha, Insight into biosorption equilibrium, kinetics and thermodynamics of crystal violet onto Ananas comosus (pineapple) leaf powder, Appl Water Sci 2 (2012) 135–141.

[39] S. Arivoli, M. Hema, P.M.D. Prasath, Adsorption of malachite green onto carbon prepared from borassus bark, The Arabian Journal for Science and Engineering 34 (2009).

[40] F. Joseph, Y.K. Agrawal, D. Rawtani, Behavior of malachite green with different adsorption matrices, Frontiers in Life Science 7 (2013) 99–111, https://doi.org/10.1080/21553769.2013.803210.

[41] A.A. Oladipo, M. Gazi, Enhanced removal of crystal violet by low cost alginate/acid activated bentonite composite beads: optimization and modelling using non-linear regression technique, Journal of Water Process Engineering 2 (2014) 43–52.

[42] B. Samiey, A.R. Toosi, Adsorption of malachite green on silica gel: effects of NaCl, pH and 2-propanol, J. Hazard. Mater. 184 (2010) 739–745.

[43] G.K. Ramesha, A. Vijaya Kumara, H.B. Muralidhara, S. Sampath, Graphene and graphene oxide as effective adsorbents toward anionic and cationic dyes, J. Colloid Interface Sci. 361 (2011) 270–277, https://doi.org/10.1016/j.jcis.2011.05.050.

[44] M.A. Hubbe, S. Azizian, S. Douven, Implications of apparent pseudo-second-order adsorption kinetics onto cellulosic materials: a review, 46 (2019).

[45] S. Lagergren, B.K. Svenska, Zur theorie der sogenannten adsorption geloester stoffe, Veternskapsakad Handlingar. 24 (1898) 1–39.

[46] Y.S. Ho, G. Mckay, Kinetic models for the sorption of dye from aqueous solution by wood, Process. Saf. Environ. Prot. 76 (1998) 183–191, https://doi.org/10.1205/095758298529326.gep.

[47] G. Crini, Kinetic and equilibrium studies on the removal of cationic dyes from aqueous solution by adsorption onto a cyclodextrin polymer, Dyes Pigments 77 (2008) 415–426, https://doi.org/10.1016/j.dyepig.2007.07.001.
[48] I. Langmuir, The adsorption of gases on plane surfaces of glass, mica and platinum, J. Am. Chem. Soc. 40 (1918) 1361–1403, https://doi.org/10.1021/ja02242a004.
[49] H.M.F. Freundlich, Over the adsorption in solution, J. Phys. Chem. 57 (1906) 385–470.
[50] V.J.P. Poots, G. McKay, J.J. Healy, Removal of basic dye from effluent using wood as an adsorbent, J. Water Pollut. Control Fed. (1978) 926–935.
[51] J.T. da Fontoura, G.S. Rolim, B. Mella, M. Farenzena, M. Gutterres, Defatted microalgal biomass as biosorbent for the removal of Acid Blue 161 dye from tannery effluent, Journal of Environmental Chemical Engineering 5 (2017) 5076–5084, https://doi.org/10.1016/j.jece.2017.09.051.